APPLICATIONS OF ELECTROPLATING METHOD FOR HEAT TRANSFER STUDIES USING ANALOGY CONCEPT

SANG-HYUK KO, DEOK-WON MOON and BUM-JIN CHUNG*
Department of Nuclear and Energy Engineering, Cheju National University
66 Jejudaehakno, Jeju-Si, Jeju-Do, 690-756, Korea
*Corresponding author. E-mail : bjchung@cheju.ac.kr

Received August 1, 2005
Accepted for Publication December 20, 2005

This study presents an idea of using analogy concept to the heat transfer studies regarding the HTGR development. Theoretical backgrounds regarding the idea were reviewed. In order to investigate the predictability of a mass transfer system for heat transfer system phenomenology, an electroplating system coupled with a limiting current technique was adopted. Test facilities for laminar forced convection and natural convections under laminar and turbulent conditions were constructed, for which heat transfer correlations are known. The test results showed a close agreement between mass transfer and heat transfer systems, which is an encouraging indication of the validity of the analogy theory and the experimental methodology adopted. This paper shows the potential of the experimental method that validates the little-understood heat transfer phenomena, even in complex geometries such as HTGR.

KEYWORDS : Analogy, Electroplating System, Limiting Current, HTGR, Mass Transfer, and Heat Transfer

1. INTRODUCTION

Hydrogen is a promising future energy source as it offers a non-petroleum-based, non-toxic, renewable, recyclable, and clean burning energy source for fuel cells, reciprocating engines and combustion turbine engines. The potential of hydrogen as an alternative energy source can help address concerns regarding global climate change, energy security and environmental air quality [1].

One of the promising production methods of hydrogen is to use the heat from an HTGR (High-Temperature Gas-cooled Reactor), a next generation nuclear reactor for a safe and reliable operation as well as for efficient and economic generation of energy [2]. As Korea has been developing its nuclear technology focusing on PWRs (Pressurized Water Reactors) with liquid-phase coolant, the development of HTGRs requires in-depth understandings of gas phase heat transfer. With HTGR, forced convection, together with the naturally-induced buoyancy force, leads to what is known as mixed convection, of which little is known. Much effort is needed to understand mixed convection as well as the variable property phenomena in order to implement the heat transfer correlations to the existing thermal hydraulics system codes.

When the buoyant effects are coupled, it is costly to obtain the heat transfer correlation experimentally. As the driving force of the flow is coupled to geometry (i.e. the facility height), reduced-scale experiments cannot possibly simulate the full-scale phenomena. In addition, with a gas coolant, due to the small heat capacity involved, heat leakages from test facility to the structural materials are inevitable; moreover, it is very difficult to extract convective heat transfer contributions as radiation heat transfers occur simultaneously.

An idea to resolve those issues is the use of the analogy concept. A heat transfer system can be transformed to a mass transfer system and vice versa. If a simple mass transfer system could be devised, and the experimental solution from that system could be obtained, then this could theoretically lead to a solution for a similar heat transfer system.

This study explores the applicability of simple mass transfer experiments to heat transfer researches using the analogy concept. Mass transfer test rigs were designed simulating well-known forced and natural convection heat transfer systems, respectively and the test results were compared with heat transfer correlations already available.

2. THEORITICAL BACKGROUND

2.1 Analogy

Analogy means likeness or similarity in structure or function. In two analogous systems, phenomenological similarity can be expected. A heat conduction problem and a mass diffusion problem with similar category of boundary and initial conditions can be an example. The

mathematical formulations for both problems are similar [3]. Thus, the heat flux can be estimated by the solution for the mass flux, and vice versa.

Table 1. Governing Equations

Heat Transfer	Mass Transfer
$\frac{\partial u}{\partial x}+\frac{\partial v}{\partial y}=0$ (Continuty equation)	
$\rho\frac{Du}{Dt}=-\frac{\partial P}{\partial x}+\mu\left(\frac{\partial^2 u}{\partial x^2}+\frac{\partial^2 u}{\partial y^2}\right)+X$ (Momentum equation)	
$\frac{DT}{Dt}=\alpha\nabla^2 T$ (Energy equation)	$\frac{DC}{Dt}=D\nabla^2 C$ (Concentration equation)

It is well known that heat transfer and mass transfer systems are completely analogous under same boundary and initial conditions as they form mathematically similar governing equations [4], neglecting the variable property effects, which is another challenging area of study. As shown in Table 1, identical governing equations are found in continuity and momentum equations, and analogous relationships are established in heat and mass transfer, respectively.

Hence, mass transfer systems can simulate heat transfer systems, or vise versa, by replacing T with C and α with D. This implies that if the bulk flow configurations are the same in both systems, and if the boundary conditions are in the same category, the heat transfer result can be obtained directly from the mass transfer result through the dimensionless group transformations (Table 2).

2.2 Electroplating Technique

Electroplating is often called electro-deposition. It is a process of producing a coating on a metallic surface by the action of electric current, and is now a conventional technique for plating gold, rhodium, nickel, tin, silver etc.

When electrical potential is applied to the copper electrodes submerged in an acidified copper sulfate solution, copper ions from the anode move to the cathode due to the electric field, copper ion density difference within the solution, and the convective motion. This results in an evenly coated layer of copper on the cathode. At this time, the electric current between the electrodes offers information about the mass transfer (Section 2.3).

Table 2. Dimensionless Group Transformations

Heat transfer	Mass transfer
Prandtl No. $\frac{\nu}{\alpha}$	Schmidt No. $\frac{\nu}{D}$
Nusselt No. $\frac{hL}{k}$	Sherwood No. $\frac{h_m L}{D}$
Rayleigh No. $\frac{g\beta H^3\Delta T}{\alpha\nu}$	$\frac{gH^3}{D\nu}\frac{\Delta\rho}{\rho}$
Reynolds No. $\frac{\bar{u}L}{\nu}$	

Levich in early 1940's introduced his electrochemical measurements on a rotating-disk electrode [7]. Agar pointed out that electrochemical mass transfer correlations should resemble closely those established for heat transfer [5, 6]. Levich further generalized his theory of applying the electrochemical method to convective diffusion [7]. Selman and Tobias summarized mass transfer correlation systematically under various conditions [8]. From then on, electrochemical measurements using the limiting current method (Section 2.4) have been used with increasing frequency and confidence in order to establish mass transfer rates at reactive surfaces in flow situations.

In this study, the copper electroplating system was employed to simulate forced and natural convection heat transfer systems, as the copper deposition has inherent advantage: copper salts, in particular *CuSO₄*, have a relati-

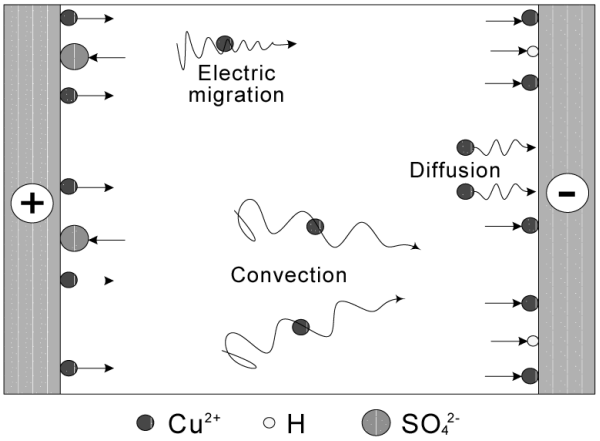

Fig. 1. Schematic Diagram of Mass Transfer in Electric Field

vely high solubility at room temperature and the electrode reaction, being a deposition reaction, does not produce a soluble product species.

2.3 Mass Transfer in Electroplating System

Figure 1 shows the movement of copper ions, which are discharged from the anode and move to the cathode when an electric potential is applied to the electrodes.

In the absence of significant temperature gradients and external accelerations other than those resulting from gravitational or electrical forces, the mass transfer of copper ions occurs through the following primary mechanisms: (1) an electric migration under a potential gradient, (2) a diffusion by ion density difference, and (3) a convective motion of solution. The total rate of transfer of a given component at a particular point within a body of solution per unit area perpendicular to the direction of transfer may be expressed by:

$$N_t = N_m + N_d + N_c \quad [kmol/m^2 \cdot s]. \tag{1}$$

where, N_t, N_m, N_d, N_c represent the total rate of the mass transfer, rate of electric migration, rate of diffusion and rate of convection, respectively [5].

For steady-state processes, it is convenient to express the rate of electric migration as a function of the current flow per unit area [9]:

$$N_m = \frac{t_n I}{nF}, \tag{2}$$

where, t_n is transference number for the given species, I is the current density (A/m^2), n is valence charge of the ion and F is the Faraday constant (96,500,000 $A \cdot s/kmol$). Thus, the quantity of electric migration can usually be evaluated from Eq. (2) and hence, may be considered separately from the diffusion and convection processes.

In simulating heat transfer systems, an electric migration doesn't appear and the convective mass transfer should concentrate on simultaneous diffusion and convection. Thus, it is convenient to define the rate of mass transfer, N_M by subtracting the electric migration rate from the total rate of transfer and the mass transfer coefficient h_m, corresponding to heat transfer coefficient, h :

$$N_M \equiv N_d + N_c = h_m (C_b - C_s). \tag{3}$$

where, C_b and C_s are the copper ion concentration in the bulk and the electrode surface, respectively. Based upon Faraday's law, the mass transfer rate N_M can be presented by

$$N_M = \frac{(1 - t_n) I}{nF}. \tag{4}$$

Thus, from Eqs. (3) and (4), h_m can be evaluated by

$$h_m = \frac{(1 - t_n) I}{nF (C_b - C_s)}. \tag{5}$$

2.4 Limiting Current Technique

For any given rate of current flow, a concentration difference corresponding to the prevailing mass transfer coefficient will be developed in the steady state between the bulk solution and surface solution on the cathode interface according to Eq. (4).

In the copper electroplating system, the interfacial reactions on the cathode are divided into two cases: the transportation of copper ions from the bulk solution to the cathode surface, and the electroplating reaction of the copper ions on the cathode surface.

The mass transfer rate, N_1 and the electroplating reaction, N_2 may be expressed as

$$N_1 = h_m (C_b - C_s) \quad \text{and} \tag{6}$$

$$N_2 = k C_s. \tag{7}$$

where, k is reaction rate constant. In steady-state, as the reaction of copper ions on the cathode holds at a constant rate, equating the Eqs. (6) and (7) leads

$$C_s = \frac{h_m C_b}{h_m + k}. \tag{8}$$

If the electric potential is increased in a given electrolytic cell, the reaction rate constant, k, will progressively increase but the mass transfer coefficient will remain constant. The increase of the potential to the cell raises the reaction rate constant to the point that the interfacial concentration can be safely regarded as zero compared to the bulk concentration, C_s as evidenced by Wike and Tobias [9]. At that time, the current does not increase but remains constant with the maximum mass transfer rate even though the applied electric potential is increased. The constant current is termed a limiting current that is determined by measuring the total polarization of the cathode in a copper electroplating system. Further increase of the potential will cause the current to increase and lead to the appearance of gas bubbles at the cathode surface due to hydrogen reduction.

Figure 2 illustrates the limiting current characteristic, which was observed experimentally for Poiseuille flow mass transfer experiment on a condition of 152 Reynolds number. Increasing the applied potential stepwise, the current increases linearly; and then limiting current is found at plateau through a monitoring of the current-potential curve.

Consequently, the limiting current technique causes it to be straightforward to measure the mass transfer rate, as the mass transfer coefficient is easily calculated without the information of the concentration at the cathode surface. At this point, Eq. (5) can be written as

$$h_m = \frac{(1-t_n)I_{\lim}}{nFC_b}. \tag{9}$$

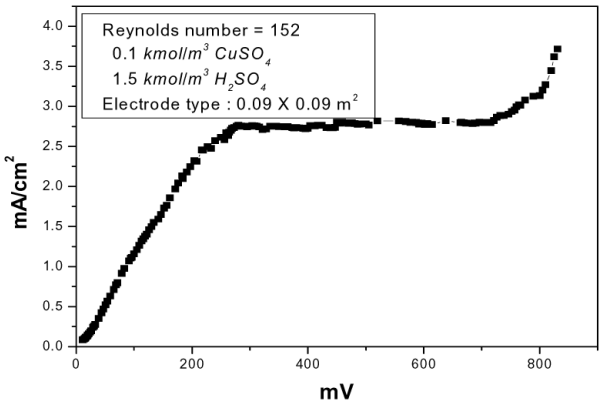

Fig. 2. Typical limiting current curve

In binary solutions, the limiting current exceeds that due to convective diffusion alone by a factor of approximately two. The excess mass transfer is caused by the electric migration of the reacting ion in the electric field, which can never be suppressed completely but can be greatly reduced by increasing the conductivity of the solution, thereby lowering the electric field strength [6]. Thus, in studies involving electrochemical mass transfer measurements, a large amount of supporting electrolyte is usually added to the solution: H_2SO_4 is added to $CuSO_4$ solution.

2.5 Dimensionless Numbers and Physical Properties

The important dimensionless groups emerging from the correlations for the mass transfer is listed in Table 2. To find out the value of these dimensionless numbers, the physical properties must be known. In this study, the empirical relations filed up by Fenech and Tobias [10] were employed, which are known to show good agreements within an error bound of 0.5% at 22°C room temperature.

$$\rho(kg/m^3) = (0.9978 + 0.06406M_H - 0.00167M_H^2 + 0.12755M_{Cu} + 0.01820M_{Cu}^2)\times 10^{-3}, \tag{10}$$

$$\mu(cp) = 0.974 + 0.1235M_H + 0.0556M_H + 0.5344M_{Cu} + 0.5356M_{Cu}^2, \tag{11}$$

$$\mu D_{Cu^{2+}}(m^2/s) = (0.7363 + 0.00511M_H + 0.02044M_{Cu})\times 10, \tag{12}$$

$$t_{Cu^{2+}} = (0.2633 - 0.1020M_H)\times M_{Cu}, \quad \text{and} \tag{13}$$

$$\frac{\rho_b - \rho_s}{\rho_b} = M_{Cu}\left(\beta_{CuSO_4} - \beta_{H_2SO_4}\frac{\Delta M_H}{\Delta M_{Cu}}\right)$$
$$\frac{\Delta M_H}{\Delta M_{Cu}} = -0.000215 + 0.113075\gamma^{1/3} + 0.85576\gamma^{2/3} - 0.50496\gamma \tag{14}$$
$$\gamma = \frac{M_{Cu}}{M_{Cu} + M_H}$$
$$\beta_j = \frac{1}{\rho}\left[\frac{\partial\rho}{\partial C_j}\right]_{T,C_k\neq j}.$$

where, M_H is the concentration of H_2SO_4 and M_{Cu} is the concentration of $CuSO_4$. A detailed description of the physical quantities is given in Table 3.

Table 3. Nomenclature

Symbol	Technical term
$\bar{u}$	Average velocity in main flow direction [m/s]
d	Channel height [m]
D	Mass diffusivity [m^2/s]
g	Gravity acceleration [9.81 m/s^2]
ρ	Density [kg/m^3]
μ	Viscosity [$kg/m\cdot s$]
t_n	Transference number

3. FORCED CONVECTION EXPERIMENTS

A few typical convective heat transfer systems were simulated by analogous mass transfer systems, and the test

results were compared with known heat transfer correlations in order to assess the accuracy of the analogy experimental method.

3.1 Poiseuille Flow

The Poiseuille flow considered in this study is a forced convection flow between two fixed, parallel and horizontal plates. The velocity profile is fully developed while the temperature profile is developing. The heat transfer correlation for the flow, averaged for the plate length, is given by [6]

$$Nu_x = 0.978\left(\mathrm{Re}\,\mathrm{Pr}\frac{d}{L}\right)^{1/3},\quad Nu_{av} = 1.467\left(\mathrm{Re}\,\mathrm{Pr}\frac{d}{L}\right)^{1/3} \tag{15}$$

where L is a electrode length, and subscript x and av denote the local and average values, respectively.

With the analogy argument, Eq. (15) can be transformed into

$$Sh_{av} = 1.467\left(\mathrm{Re}\,Sc\frac{d}{L}\right)^{1/3}. \tag{16}$$

One of the limitations of this electrochemical measurement is that the local mass transfer rate is difficult to measure, as it only measures the total current in the cell. In order to overcome this limitation, the measurements of local mass transfer rates were also performed using piecewise electrodes. Eq. (17) expresses the local mass transfer Sherwood number from length L_{i-1} to L_i :

$$Sh_{local} = \frac{1}{L_i - L_{i-1}}\int_{L_{i-1}}^{L_i} Sh_x dx = 1.467\left(\mathrm{Re}\,Sc\frac{d}{\overline{x}_i}\right)^{1/3}$$

$$\text{where, } \overline{x}_i = \left[\frac{L_i - L_{i-1}}{L_i^{2/3} - L_{i-1}^{2/3}}\right]. \tag{17}$$

3.2 Test Facility

Figure 3 shows the test facility. The plate to plate spacing is 0.02 *m* and the 0.7 *m* entrance length ensures a fully developed laminar flow over the electrodes. The flow rate at the test section is adjusted by controlling the head between upstream and downstream reservoir using valves. The fluid from downstream reservoir is recycled to upstream reservoir by a magnetic pump.

The electric potential to the test section was applied using D.C. power supply (Toyotech DP30-05A) and controlled by a variable resistor (RU-410B). Then the currents between the electrodes were measured by Dual Display Multimeter (Fluke-45) under various flow rates.

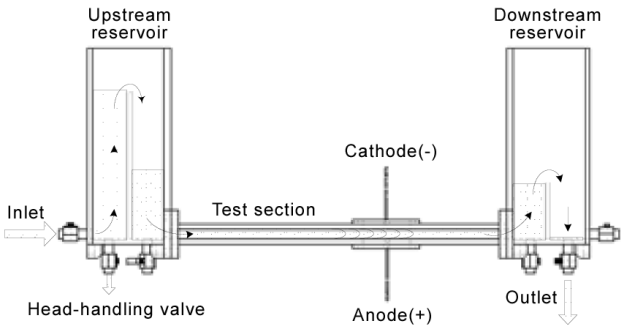

Fig. 3. Conceptual Diagram for Poiseuille Flow Experiments

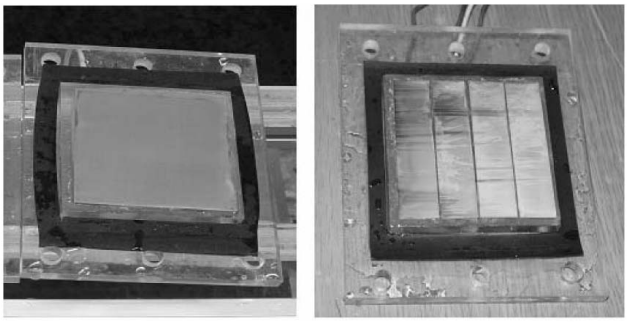

Fig. 4. Cupric Electrodes for Average and Local Mass Transfer

The copper electrodes are 0.09 *m* wide and 0.09 *m* long and embedded in the horizontal walls of a 1.3 *m* long rectangular test section facing each other. The electrodes are very thin copper plate so that the applied electric potential in the whole range of the plate is the same. The electrolyte consists of 0.1 *kmol/m³* $CuSO_4$ solutions with 1.5 *kmol/m³* H_2SO_4 as a supporting electrolyte.

Figure 4 displays the copper electrodes used in the test facility. The piece-wise electrodes were composed of four pieces of electrodes, each 0.022 *m* long, set in a line to the flow direction with 1 mm epoxy insulations among them.

3.3 Results and Discussions

With the fixed electrolyte concentrations of 1.5 *kmol/m³* H_2SO_4 and 0.1 *kmol/m³* $CuSO_4$, the Schmidt number is a constant of 2,094 and only the flow velocity was controllable. The Reynolds number varied from 18 to 400. For a specific Reynolds number, the currents were measured increasing the applied potential until the plateau appeared.

The test results for the average mass transfer are preented in Fig. 5. The mass transfer test results show good agreement with the known heat transfer correlation of Eq. (16), and the maximum error was within 5%. Generally, the higher the Reynolds number, the higher the limiting current that was measured.

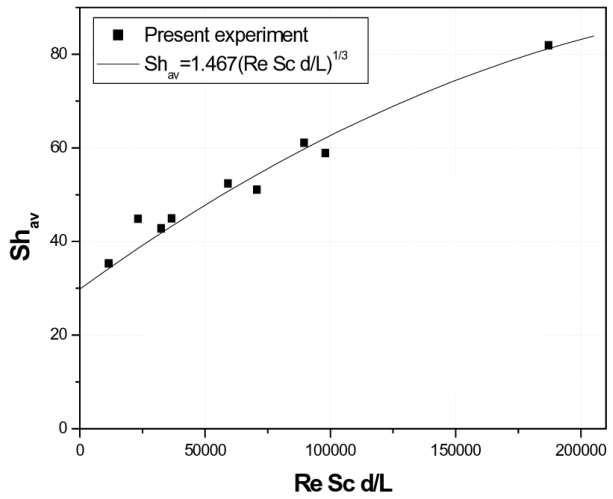

Fig. 5. Test Results for the Measured Average Mass Transfer Rate

Figure 6 illustrates the local mass transfer test results. The test results that utilized the piece-wise electrode showed good agreement with the correlation, within an error bound of 10%.

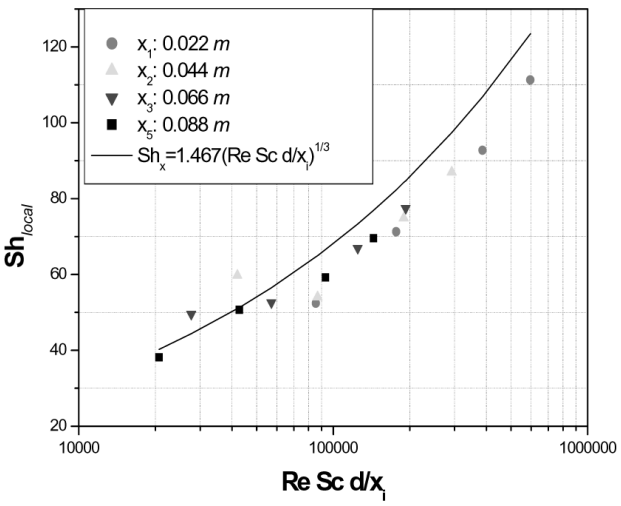

Fig. 6. Test Results for the Measured Local Mass Transfer Rate

4. NATURAL CONVECTION EXPERIMENTS

4.1 Natural Convection at Vertical Plates

A natural convection differs fundamentally from a forced convection. Flow is driven by buoyancy due to the presence of gravitational acceleration and density variations. The flow field is intimately coupled to the temperature field in a heat transfer system.

The natural convection heat transfer correlation [4] under the laminar condition, obtained by a similarity solution, is again easily converted to a mass transfer correlation with a dimensionless numbers transformation:

$$Nu = 0.66(Gr\,\mathrm{Pr})^{1/4} \quad \text{and} \tag{18}$$

$$Sh = 0.66(GrSc)^{1/4} \text{ at } \; Gr < 10^9 . \tag{19}$$

As for a turbulent natural convection, the mass transfer expression can be readily established with the same approach [6]:

$$Sh = 0.31(GrSc)^{0.28} \quad \text{at} \quad Gr > 10^9 . \tag{20}$$

4.2 Test Facility

Figure 7 shows the experimental facility that simulates the buoyancy-driven flows. The electrolytic cell was a rectangular Lucite container of 0.15 *m* wide, 0.4 *m* high and 0.3 *m* long. The anode and the cathode were vertical copper plates of 0.12 *m* wide, and were fitted exactly into the electrolytic cell.

In order to simulate both laminar and turbulent natural convections, two different heights of 0.1 *m* and 0.28 *m*, were adopted to achieve the corresponding Grashof or Rayleigh numbers, which require about 0.5 *m* high and 10 *m* high natural convection heat transfer systems of air, respectively.

With fixed H_2SO_4 concentrations of 1.5 *kmol/m*^{3}, $CuSO_4$ concentrations varied from 0.01 to 2.5 *kmol/m*^{3}. The test

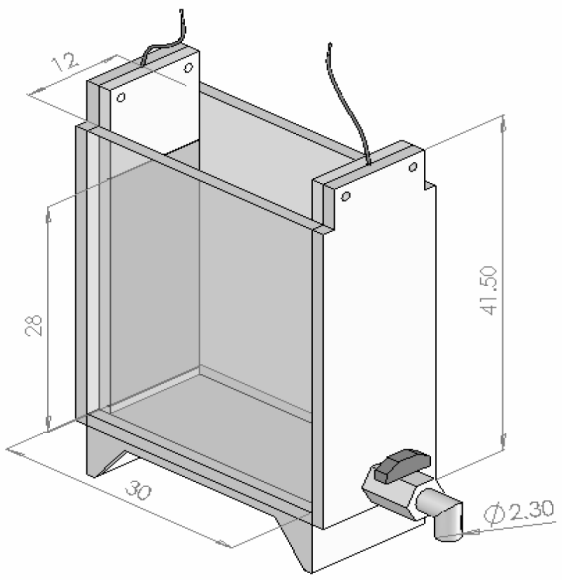

Fig. 7. Natural Convection Test Facility

conditions for laminar and the turbulent natural convections are summarized in appendix.

The heated wall was simulated by the cathode as in the electroplating system depletion; the buoyancy was induced by the copper ion density.

4.3 Results and Discussions

The measurement of the natural convection mass transfer rate with the height of 0.1 *m* electrodes was accomplished for various ranges of Grashof and Schmidt numbers varying the cupric sulfate concentration. The test results over a range of Schmidt number from 1960 to 2280 and over a range of Grashof number from 8.83×10^6 to 1.48×10^8, which are regarded laminar flow conditions, were in good agreement with the correlation (19).

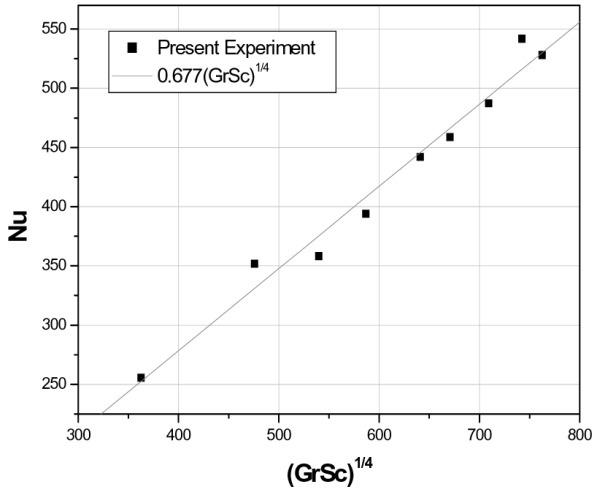

Fig. 9. Natural Convection Test Results Under the Laminar Condition

For turbulent natural convection, mass transfer experiments were carried out using the electrodes with a 0.28 *m* height with three different anode types. Figure 10 shows that the agreement of experimental data is remarkably good. Test results also show that the mass transfer relations measured are insensitive to the anode geometry and size, as the transfer characteristics were mainly determined at the cathode surface.

5. CONCLUSIONS

In order to explore the applicability of an analogy concept to the HTGR heat transfer studies, an electroplating system with a limiting current technique was adopted. Three different forced and natural convection mass transfer systems were constructed in order to simulate a Poiseuille flow at a horizontal geometry and laminar and turbulent buoyant flows at a vertical geometry.

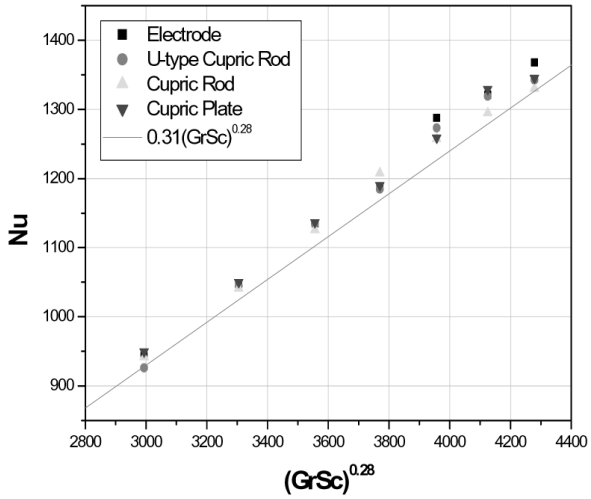

Fig. 10. Natural Convection Test Results Under the Turbulent Condition

The validity of the analogy experimental method was confirmed through comparisons between the test results and corresponding well-known heat transfer correlations. It was shown that there exists a close agreement between the results for the mass transfer experiment and the heat transfer correlation; this is an encouraging indication of the validity of the analogy theory and the experiment method. It may also be concluded that analogy method using the electroplating system makes it possible to predict the unknown heat transfer correlations. In addition, it was found that high Grashof or Rayleigh numbers can be achieved by a short test facility of about 1/50 for natural convection heat transfer systems of gas. Thus, the analogy methodology is expected to help address the examination of heat phenomena for HTGR development, as the electroplating method not only provides useful information regarding heat transfers but also has a cost-effective advantage over any other comparable experimental method. It was also found that the flow is visualized depending on the copper ion concentration.

ACKNOWLEDGEMENTS

This work is supported by the Nuclear Academic Research Program of the Ministry of Science and Technology (MOST).

REFERENCES

[1] Seaworthy System Inc., “One-demand Hydrogen Generating System Demonstration Concept Development,” PHASE I: TASK 5.0 : Final report, Center for Commercial Deployment of Transportation Technology(2002).

[2] Jong-Hwa Jang, et al., “Basic Study on High Temperature Gas-Cooled Reactor Technology for Hydrogen Production,” RR-2435, Korea Atomic Energy Research Institute(2003).

[3] G. Murphy, *Similitude in Engineering*, New York, Ronald

Press(1950).
[4] A. Bejan, *Convection Heat Transfer*, **2nd ed**., p. 466-514, New York, John Wiley & Sons, INC.(1994).
[5] J. N. Agar, "Diffusion and Convection at Electrodes," *Discussion of Faraday Soc*., **1**, pp.27-37, 1947.
[6] Thomas B. Drew, et al., *Advances in Chemical Engineering*, Academic Press, New York · London, **10**, p211-336(1978).
[7] V. G. Levich, *Physicochemical Hydrodynamics*, Prentice-Hall, Englewood (1962).
[8] J. R. Selman and C. W. Tobias, "Mass Transfer Measurement by the Limiting Current Technique," *Adv. Chem. Eng*., **10**, pp.211-318 (1978).
[9] C. R. Wike and C. W. Tobias, et al., "Free-Convection Mass Transfer at Vertical Plates," *Chemical Engineering Progress*, **49**, No. 12, p663-674(1953).
[10] E. J. Fenech and C. W. Tobias, "Mass Transfer by Free Convection at Horizontal Electrodes," *Electrochemical Acta*, **2**, p311-325(1960).

APPENDIX

Table A-1 Test Matrix for Natural Convection Under Laminar Condition

$CuSO_4$ $(kmol/m^3)$	ρ (kg/m^3)	μ $(kg/m\cdot s)$ $\times10^{-3}$	D (m^2/s) $\times10^{10}$	t_n $\times10^{-4}$	$\frac{\rho_b-\rho_s}{\rho_b}$ $\times10^{-4}$	Gr $\times10^{6}$	Sc	$(GrSc)^{1/4}$
0.01	1091	1.23	5.77	11.03	11.47	8.83	1957	362.6
0.03	1094	1.24	5.72	33.09	33.95	25.83	1984	475.8
0.05	1096	1.25	5.67	55.15	56.15	42.17	2014	539.9
0.07	1099	1.26	5.63	77.21	78.18	57.94	2045	586.7
0.10	1103	1.28	5.55	110.3	111.10	80.58	2094	640.9
0.12	1105	1.29	5.50	132.4	132.93	95.05	2128	670.7
0.15	1109	1.31	5.43	165.5	177.72	115.82	2183	709.1
0.18	1113	1.33	5.35	198.5	198.57	135.51	2242	742.4
0.20	1116	1.34	5.29	220.6	220.34	148.04	2282	762.5

Table A-2 Test Matrix for Natural Convection Under Turbulent Condition

$CuSO_4$ $(kmol/m^3)$	ρ (kg/m^3)	μ $(kg/m\cdot s)$ $\times10^{-3}$	D (m^2/s) $\times10^{10}$	t_n $\times10^{-4}$	$\frac{\rho_b-\rho_s}{\rho_b}$ $\times10^{-4}$	Gr $\times10^{9}$	Sc	$(GrSc)^{0.28}$
0.07	1099	1.26	5.63	77.21	78.19	1.27	2045	2993
0.10	1103	1.27	5.55	110.3	111.1	1.77	2094	3306
0.13	1107	1.29	5.48	143.4	143.8	2.24	2147	3557
0.16	1111	1.31	5.40	176.5	176.6	2.69	2202	3770
0.19	1115	1.33	5.32	209.6	209.4	3.11	2262	3957
0.22	1119	1.36	5.24	242.7	242.3	3.51	2325	4125
0.25	1123	1.38	5.16	275.7	275.3	3.89	2392	4279